Development of GaN-Based Vertical-Cavity Surface-Emitting Lasers

Tien-Chang Lu, *Member, IEEE*, Jun-Rong Chen, Shih-Wei Chen, Hao-Chung Kuo, *Senior Member, IEEE*, Chien-Cheng Kuo, Cheng-Chung Lee, and Shing-Chung Wang, *Life Member, IEEE*

(Invited Paper)

***Abstract*—This paper reviews the fabrication technology and performance characteristics of optically pumped and electrically pumped GaN-based vertical-cavity surface-emitting lasers (VCSELs). The lasing action of optically pumped hybrid GaN-based VCSELs has been observed at room temperature due to the employment of high-quality and high-reflectivity AlN/GaN-based distributed Bragg reflectors in the VCSEL structure. Based on the device structure of the optically pumped hybrid GaN-based VCSELs, we further achieved the lasing action of electrically pumped GaN-based VCSELs under continuous-wave operation at 77 K. The laser has a threshold injection current of 1.4 mA and emits a blue wavelength at 462 nm together with a narrow linewidth of about 0.15 nm. The laser beam has a divergence angle of about 11.7° with a polarization ratio of 80%. A very strong spontaneous coupling efficiency of 7.5×10^{-2} was measured.**

***Index Terms*—Distributed Bragg reflector (DBR), GaN, electrical pumping, superlattice, vertical-cavity surface-emitting laser (VCSEL).**

I. Introduction

NITRIDE-BASED wide-bandgap alloys such as InGaN and AlGaN have been used in the fabrication of light-emitting devices including LEDs, laser diodes (LDs), and vertical-cavity surface-emitting lasers (VCSELs). Early breakthroughs for III-nitride LEDs can be traced back to the experimental results demonstrated by Akasaki and coworkers. In 1989, they obtained p-type GaN films by using Mg doping as an acceptor impurity. The Mg acceptors were activated by post-low-energy electron beam irradiation treatment [1]. Subsequent to the realization of p-type conductivity in GaN, the first GaN-based homojunction LED was also reported by Akasaki *et al.* [2]. Furthermore, high-brightness InGaN/GaN LEDs based on double-heterostructure design were demonstrated by Nakamura *et al.* [3], and then the related ultraviolet, blue, green, and yellow LEDs were commercialized in the following years. The GaN-based LDs were also realized under room-temperature (RT) continuous-wave (CW) operation by Nakamura *et al.* [4]. The lifetime and output power of the LDs were further improved to more than 10 000 h and 420 mW in 1998 [5], [6]. These breakthroughs are mainly based on the improvement of crystal quality and the realization of further p-type conductivity control [7], [8]. Nevertheless, the development of GaN-based VCSELs is relatively slow as compared with GaN-based LEDs and LDs. The key problems limiting the development of GaN-based VCSELs are the lack of suitable substrates and the difficulty in growing high-quality and high-reflectivity GaN-based distributed Bragg reflectors (DBRs). In Section II, we will describe the difficulty in growing and fabricating GaN-based VCSELs in detail, and propose the corresponding approach to these problems.

VCSELS have many inherent advantages, such as circular output beam, low beam divergence, high modulation bandwidth, single longitudinal mode, and convenient wafer-level testing [9]–[11]. These advantages make VCSELs promising optoelectronic devices for many practical applications, such as high-density optical storage system, laser printing, free-space optical interconnects, fiber-optic communications, etc. Recently, nitride-based VCSEL microcavities have especially attracted much attention due to the investigation of fundamental phenomena including strong light–matter interaction [12]–[14], solid-state cavity quantum electrodynamics (CQED) [15], and dynamical Bose–Einstein condensates [16]. Because of the desirable breakthrough in the realization of GaN-based VCSELs and the related study of GaN-based microcavities, there are many research groups devoted to the growth and fabrication of GaN-based VCSELs. Despite the material quality and fabrication problems, realizations of the GaN-based VCSELs have been reported. The first demonstration of the RT optically pumped GaN-based VCSELs has been reported by Redwing *et al.* [17]. The fully epitaxial VCSEL structure consists of a 10 μm GaN active region sandwiched between 30-period $Al_{0.12}Ga_{0.88}N/Al_{0.4}Ga_{0.6}N$-based DBRs with the reflectivity values about 84%–93% from theoretical prediction. The relatively low reflectivity results in the high-threshold pumping energy of $\sim$2.0 MW/cm^2 and the employment of a thick GaN gain layer. Furthermore, Arakawa and coworkers fabricated an $In_{0.1}Ga_{0.9}N$ VCSEL and observed the lasing action at 77 K for the first time in 1998 [18]. The 3λ cavity

Manuscript received November 1, 2008; revised December 11, 2008. First published February 10, 2009; current version published June 5, 2009. This work was supported in part by the Ministry of Education Aiming for Top University (MOE ATU) Program and in part by the National Science Council of the Republic of China under Contract NSC 96-2221-E009-092-MY3, Contract NSC 96-2221-E009-093-MY3, and Contract NSC 96-2221-E009-094-MY3.

T.-C. Lu, J.-R. Chen, S.-W. Chen, H.-C. Kuo, and S.-C. Wang are with the Department of Photonics and the Institute of Electro-Optical Engineering, National Chiao Tung University (NCTU), Hsinchu 30050, Taiwan (e-mail: timtclu@faculty.nctu.edu.tw; jrchen.eo95g@nctu.edu.tw; macub.eo95g@nctu.edu.tw; hckuo@faculty.nctu.edu.tw).

C.-C. Kuo is with the Thin Film Technology Center, National Central University (NCU), Jhongli 32001, Taiwan (e-mail: cckuo@dop.ncu.edu.tw).

C.-C. Lee is with the Department of Optics and Photonics, National Central University (NCU), Jhongli 32001, Taiwan (e-mail: cclee@dop.ncu.edu.tw).

Color versions of one or more of the figures in this paper are available online at http://ieeexplore.ieee.org.

Digital Object Identifier 10.1109/JSTQE.2009.2013181

1077-260X/$25.00 © 2009 IEEE

comprising an $In_{0.1}Ga_{0.9}N$ active layer was grown on 35-pair $Al_{0.34}Ga_{0.66}N$/GaN-based DBRs with the reflectivity of 97%. The top DBR consisting of a six-pair TiO_2/SiO_2 multilayer providing the reflectivity of 98% was evaporated on the top of the active layer to form the hybrid VCSEL structure (i.e., the VCSEL structure consisting of semiconductor-grown mirror and dielectric-deposited mirror). The emission linewidth significantly decreased from 2.5 to 0.1 nm after the threshold condition. Thereafter, Song *et al.* demonstrated a VCSEL structure consisting of InGaN multiple quantum wells (MQWs) and ten-pair SiO_2/HfO_2 top and bottom DBR by using laser lift-off technology [19]. Since the reflectivity of top and bottom DBRs were 99.5% and 99.9%, respectively, the cavity Q-factor is larger than 600 in their experiments. In the same year, Someya *et al.* reported RT lasing at blue wavelengths in hybrid GaN-based VCSELs [20]. Lasing action was observed at a wavelength of 399 nm under optical excitation and the emission linewidth decreased from 0.8 nm below threshold to less than 0.1 nm above threshold. In 2005, crack-free fully epitaxial nitride microcavity using lattice-matched AlInN/GaN-based DBRs was reported by Carlin *et al.* [21]. The optical cavity was formed by a $3\lambda/2$ GaN cavity surrounded by lattice-matched AlInN/GaN-based DBRs with reflectivity values close to 99%. The cavity mode was clearly resolved with a linewidth of 2.3 nm. However, laser behavior was not reported in this kind of VCSEL structure at that time.

As far as optically pumped GaN-based VCSELs are concerned, there are only few experimental results in recent years [22]–[25]. In our previous study, we also demonstrated optically pumped GaN-based VCSELs by employing dielectric DBR VCSEL [26], [27] and hybrid DBR VCSEL structures [28], [29]. The advantages and drawbacks of these different VCSEL structures will be discussed in Section II. The related technology and characteristics of optically pumped GaN-based VCSELs can be found in the published review paper [30]. Although optically pumped GaN-based VCSELs were reported earlier, there has been no electrically pumped GaN-based VCSEL reported until our recent experimental results exhibiting the lasing action at 77 K [31]. In Section III, we will focus on the hybrid VCSEL structure and discuss the characteristics of optically pumped and electrically pumped GaN-based VCSELs. In Section IV, the future research directions enhancing the operation temperature from 77 to 300 K will be discussed. Section V presents a summary of this paper and discusses the emerging applications for nitride-based VCSELs.

II. Difficulty in Fabrication of Nitride-Based VCSEL

The evolution of nitride-based light-emitting devices suffered from many obstacles, such as the absence of lattice-matched substrates [32], low activation ratio of p-type (Al)GaN [33], large mobility difference between electrons and holes [34], crystal-structure- and strain-induced quantum-confined Stark effect (QCSE) [35], etc. These problems have been widely investigated in nitride-based LEDs and LDs. Nevertheless, the most difficult challenge for nitride-based VCSELs is the lattice-mismatched nitride-based DBRs since the VCSEL structure consists of an active region embedded within two high-reflectivity DBRs. High-quality and high-reflectivity DBRs are necessary to achieve threshold condition due to the relatively short gain region of a VCSEL [9], [10]. In general, there are three kinds of material systems used in nitride-based DBRs, including AlN/GaN, Al(Ga)N/(Al)GaN, and AlInN/GaN. The AlN/GaN-based DBRs offer the highest refractive index contrast among the III-nitride compounds and provide highly reflective structures together with a large stopband width. However, the large lattice mismatch between AlN and GaN is up to 2.4%, which generally results in tensile strain and formation of cracks. These cracks tend to grow into V-shaped grooves and seriously affect the reflectivity of the DBR due to scattering, diffraction, and absorption. To prevent the formation of cracks, the $Al_xGa_{1-x}N/Al_yGa_{1-y}N$ system is usually used to reduce the strain in the whole DBR structure. Nevertheless, the refractive index contrast decreases with increasing Al composition in GaN or Ga composition in AlN, which leads to a reduced stopband width and the requirement of increased number of pairs to achieve high reflectivity. An alternative approach was proposed by Carlin and Ilegems [36]. They demonstrated high-reflectivity AlInN/GaN-based DBRs near-lattice-matched to GaN. The 20-pair DBRs exhibited a peak reflectivity of over 90% and a 35 nm stopband width at 515 nm. Although this kind of DBR has been reported, the growth of high-quality AlInN film is difficult due to the composition inhomogeneity and phase separation in AlInN, which results from large mismatch of covalent bond length and growth temperature between InN and AlN [37]. The related progress in the growth of highly reflective nitride-based DBR can be found in the review paper [38].

In order to obtain high-reflectivity and large-stopband DBRs for nitride-based VCSELs, our approach is to focus on growing high-quality AlN/GaN-based DBRs. In our previous study, we reported the growth of crack-free AlN/GaN-based DBRs with insertion of 5.5 periods of AlN/GaN superlattice (SL) [39]. Fig. 1 shows cross-sectional transmission electronic microscopy (TEM) images of the SL DBR structure. The lighter layers represent AlN layers while the darker ones represent GaN layers. The interfaces between AlN and GaN layers are sharp and abrupt in low-magnification TEM image, as shown in Fig. 1(a). The arrows indicate the SL insertion positions. Fig. 1(b) shows the cross-sectional TEM image of one set of 5.5-pair AlN/GaN SL insertion layers under high magnification. Detailed observations by this TEM image reveal that the V-shaped defects in the AlN layers are always observable at the GaN-on-AlN interfaces and are filled in with GaN. These V-shaped defects have been reported earlier and could be due to various origins such as stacking mismatch boundaries and surface undulation [40]. The GaN/AlN SL insertion layers were followed by one more AlN layer to identify the change from the AlN layer to the GaN layer. Here, a set of GaN/AlN SL insertion layers can be seen as a quasi-alloy of an $Al_xGa_{1-x}N$ layer for a low-refractive-index quarter-wave layer in the DBR structure.

The effect of the SL insertion layers on the structural characteristics of the DBR structures can be investigated by the measurement of X-ray asymmetrical reciprocal space map (RSM). The $(1\,0\,\bar{1}\,5)$ RSMs of the AlN/GaN-based DBRs without and

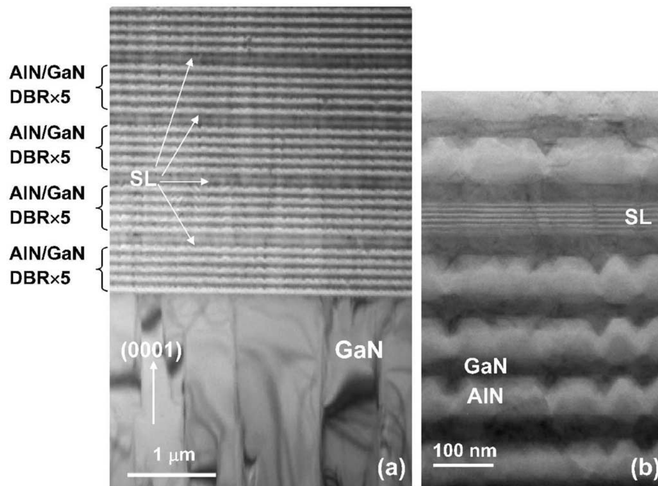

Fig. 1. (a) Low-magnification cross-sectional TEM image of the SL DBR structure. (b) High-magnification cross-sectional TEM image of the SL DBR structure. The 5.5-pair AlN/GaN SL can be observed clearly.

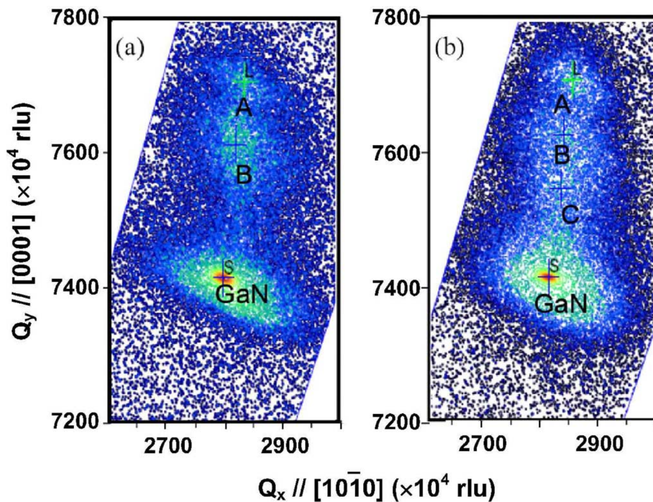

Fig. 2. Reciprocal space maps. (a) Non-SL samples. (b) SL DBR samples.

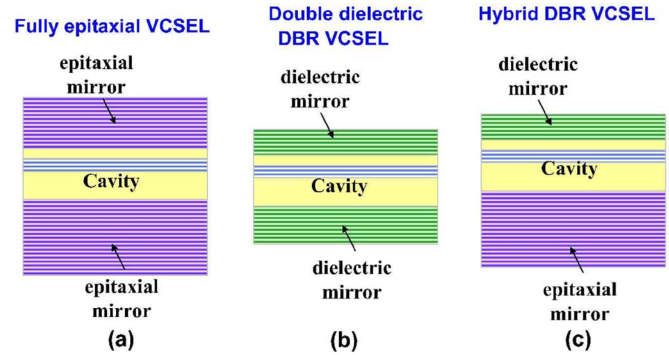

Fig. 3. Three kinds of GaN-based VCSEL structures. (a) Fully epitaxial VCSELs. (b) Double dielectric DBR VCSELs. (c) Hybrid DBR VCSELs.

with SL insertion layers are shown in Fig. 2(a) and (b), respectively. The perpendicular axis represents the reciprocal lattice c and the parallel axis represents reciprocal lattice a. Compared with the RSM patterns of non-SL and SL DBRs in Fig. 2(a) and (b), the diffraction patterns around spots labeled A and B are due to the DBR layers for the high aluminum composition. The diffraction spot labeled C is due to the AlN/GaN SL insertion layers, as shown in Fig. 2(b). Both RSM patterns in non-SL and SL DBRs reveal that the DBR layers are under tensile strain that is partially relaxed because the diffraction peaks in the $(10\bar{1}5)$ RSMs do not align in a vertical straight line. The relaxation could be due to the creation of the misfit dislocation [40]. The relaxation process of AlN/GaN SL layers ensures relatively better coherency, i.e., GaN and AlN SL layers are fully strained against each other. Therefore, the SLs behave like effective bulk layers that have an in-plane lattice constant between bulk GaN- and AlN-based DBR layers, as shown in Fig. 2(b) [41]. The subsequent growth of five-pair AlN/GaN-based DBR could follow the AlN/GaN SLs, which will make the DBR layers suffer relatively smaller strain as compared with DBR layers grown on bulk GaN layers. Consequently, the insertion of the SL layers during the growth of the DBR layers could act as a strain buffers between DBRs and the underlying GaN bulk layer because the in-plane lattice constants of the SL layers are close to those of the AlN layers in the DBRs.

Because of the difficulty of growing high-quality and high-reflectivity nitride-based DBRs, the possible design of GaN-based blue VCSELs has been proposed by Iga [42]. The corresponding structural designs for nitride-based VCSELs can be classified into three major types, as shown in Fig. 3. The first one is monolithic-grown vertical resonant cavity consisting of epitaxially grown III-nitride top and bottom DBRs [Fig. 3(a)]. The advantage of the fully epitaxial microcavity is the controllable cavity thickness, which is beneficial to fabricate a microcavity structure. However, VCSELs require extremely high-reflectivity DBRs (i.e., high cavity Q-factor). It is very difficult for the fully epitaxial nitride double dielectric microcavity to achieve this requirement although the related results have been reported [21], [43]. The second one is vertical resonant cavity consisting of a dielectric top and bottom DBR [Fig. 3(b)]. The DBR VCSELs can exhibit high cavity Q-factors because of the high-reflectivity DBRs, which are relatively easy to fabricate. The large refractive index contrast in dielectric materials can provide high-reflectivity and large-stopband DBRs with less number of pairs. The drawbacks of the double dielectric DBR VCSEL are the difficulty of controlling the cavity thickness precisely and the complicated fabrication process due to the employment of laser lift-off technique [26]. In addition, the GaN cavity should be kept as thick as possible to avoid the damage of the InGaN/GaN MQWs during the laser lift-off process. Such a thick cavity length could increase the threshold condition and reduce the microcavity effect [44], [45]. The third one is the VCSEL structure combining an epitaxially grown DBR and a dielectric-type DBR that compromises the advantages and disadvantages of the aforementioned two VCSEL structures [Fig. 3(c)] [28], [29]. The hybrid DBR VCSEL can eliminate the complex process and ensure the feasibility of coplanar contacts with dielectric DBR mesas for the future electrically pumped VCSEL applications. The major requirement for the fabrication

of hybrid DBR VCSEL is to grow high-reflectivity and high-quality nitride-based DBRs. Our approaches to the realization of GaN-based VCSELs are mainly based on the double dielectric DBR VCSELs and the hybrid DBR VCSELs. The lasing action in double dielectric VCSEL has been demonstrated by optical excitation in our previous studies [26], [27]. To achieve electrically pumped GaN-based VCSELs, we focus our study on the structure of hybrid DBR VCSELs in recent years. Since the problem of growing high-reflectivity nitride-based DBRs has been successfully overcome by inserting the AlN/GaN SL layers during the growth of AlN/GaN-based DBRs, it is expected that the higher possibility for achieving electrically pumped GaN-based VCSELs is based on the hybrid DBR VCSEL structure. Therefore, we will analyze the performance characteristics of optically pumped and electrically pumped GaN-based hybrid VCSELs in the following section.

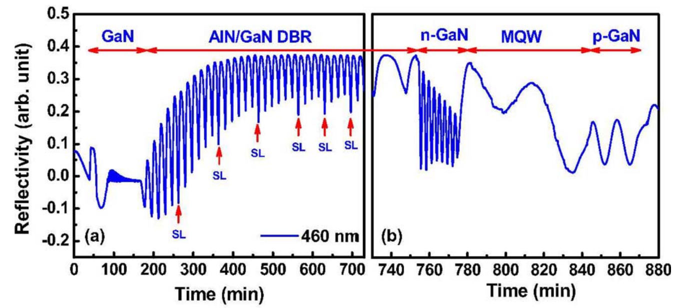

Fig. 4. (a) *In situ* normal reflectance measurement during the growth of the AlN/GaN-based DBR and GaN microcavity with InGaN/GaN MQWs by a fixed measurement wavelength of 450 nm. The AlN/GaN SL s are inserted into AlN/GaN-based DBR at the time indicated as SL. (b) Enlarged part of reflectance signals during the growth of the GaN microcavity consisted of n-GaN, InGaN/GaN MQWs, and p-GaN layers.

III. Hybrid Nitride-Based VCSEL

A. Growth and Fabrication of Hybrid DBR VCSEL

The hybrid DBR GaN-based VCSELs were grown in a low-pressure high-speed rotating disk metal–organic chemical vapor deposition (MOCVD) system (EMCORE D75). Two-inch-diameter (0 0 0 1)-oriented sapphire substrates were used for the growth of AlN/GaN-based DBR and cavity. During the growth, trimethylgallium (TMGa), trimethylindium (TMIn), and trimethylaluminum (TMAl) were used as group III source materials, and ammonia (NH_3) as the group V source material. Then, the growth process was as follows. The substrate was thermally cleaned in hydrogen ambient for 5 min at 1100 °C and then a 30-nm-thick GaN nucleation layer was grown at 500 °C. The growth temperature was raised up to 1100 °C for the growth of a 2-μm GaN buffer layer. Then, the 29 pairs of AlN/GaN-based DBR with six AlN/GaN SL insertion layers were grown under the fixed chamber pressure of 100 torr similar to the previously reported growth conditions [39]. In order to reduce the tensile strain between the AlN and GaN, we inserted one SL into each of the five DBR periods for the first 20 pairs of DBRs. Then, the SL was inserted into each of the three DBR periods for the remaining nine pairs of DBRs so as to reduce the tensile strain. The overall AlN/GaN-based DBRs have 29 pairs with six SL insertion layers. On top of this, the 29-pair AlN/GaN-based DBR is a 790-nm-thick Si-doped n-type GaN cladding layer. The MQW active region consists of ten 2.5-nm-thick $In_{0.2}Ga_{0.8}N$ QWs and 7.5-nm-thick GaN barrier layers. A 120-nm-thick Mg-doped p-type GaN cladding layer was grown on top of the MQWs to form a 5λ cavity in optical thickness for a center wavelength of 460 nm. Here, we chose 460 nm as the designed lasing wavelength mainly due to the consideration of the higher absorption of the Indium-Tin-Oxide (ITO) layer at shorter wavelengths. Besides, this wavelength can be supported by our *in situ* monitor system, which is a very critical consideration for the precise design of each layer thickness in VCSEL structures [9]. The MQWs were located at the antinode of light field in the microcavity for enhancing the coupling of photons and the cavity mode. During the growth, we use *in situ* monitoring signals by fixing the monitor wavelength of 460 nm. Therefore, the thickness of each quarter-wavelength GaN and AlN can be precisely controlled by following the reflectance signals during the MOCVD growth. The total reflectance signal at 460 nm for the half-cavity structure is shown in Fig. 4. The relative reflectivity is gradually saturated with increasing number of DBR pairs, as shown in Fig. 4(a). The AlN/GaN SL layers are inserted into AlN/GaN-based DBR at the time indicated as SL. The cavity thickness and positions of MQWs can also be *in situ* monitored by observing the oscillation periods during the growth, as shown in Fig. 4(b). After the growth of nitride-based half cavity, an eight-pair Ta_2O_5/SiO_2 dielectric mirror was deposited by electronic beam evaporation as the top DBR reflector to form the hybrid microcavity.

B. Characteristics of Optically Pumped GaN-Based VCSEL

Lasing action observed by optical pumping is the first step for the development of semiconductor lasers. The experimental results obtained from optically pumped VCSELs can be used to estimate the threshold condition of the designed VCSEL structure and provide better understanding of the material properties. First, we examined the reflectivity spectrum of the full VCSEL structure, which can assure the accuracy of the cavity thickness. Fig. 5 shows the RT reflectivity spectrum of whole microcavity under near-normal incidence. The peak reflectivity is about 97% with a large stopband of 70 nm originating from the large refractive index contrast between Ta_2O_5 and SiO_2 layers. The irregular long-wavelength oscillations of the reflectivity spectrum arise from the modulation of the respective top and bottom DBR spectra. On the other hand, the short-wavelength oscillator is relatively regular, which only results from the top dielectric DBR, since the short-wavelength light is absorbed by the GaN layer. The photoluminescence (PL) emission spectrum of the full microcavity was measured at RT, and shown in Fig. 5 as well. The excitation source is a 325-nm He–Cd laser. In Fig. 5, the cavity resonance mode at 464.2 nm with a full-width at half-maximum (FWHM) value of 0.61 nm is clearly observed. The cavity mode dip is located at the reflectivity curve corresponding to the emission peak. This indicates that the InGaN/GaN MQWs emission peak was well aligned with the hybrid

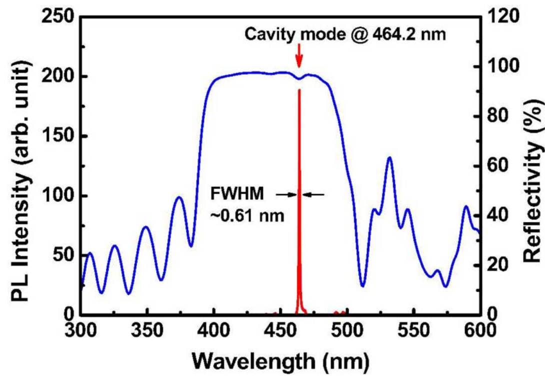

Fig. 5. RT reflectivity spectrum and PL spectrum of whole GaN-based microcavity.

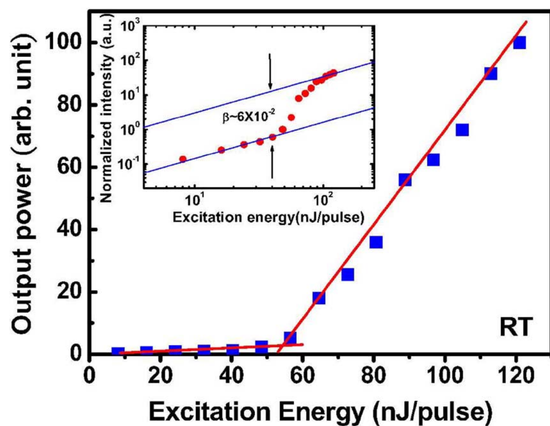

Fig. 6. Laser emission intensity as a function of the exciting energy at RT conditions for hybrid DBR VCSEL.

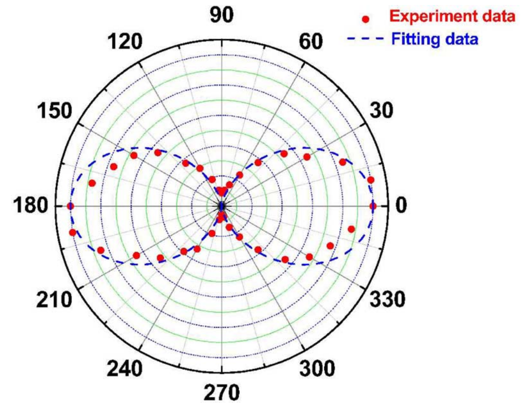

Fig. 7. Polarization characteristic of the laser emission at the pumping energy of 82.5 nJ for the hybrid DBR VCSEL. The solid dot shows the experiment data and the dashed line shows the fitting curve.

microcavity. The cavity Q-factor was estimated from the $\lambda/\Delta\lambda$ to be about 760.

To examine the lasing action, we measured the emission intensity of the hybrid microcavity with increasing pumping power using a microscopic optical pumping system. The optical pumping of the samples was performed using a frequency-tripled Nd:YVO_4 355-nm pulsed laser with a pulsewidth of $\sim$0.5 nm at a repetition rate of 1 kHz. The pumping laser beam with a spot size ranging from 30 to 60 μm was incident normal to the VCSEL sample surface. The light emission from the VCSEL sample was collected using an imaging optic into a spectrometer/charge-coupled device (CCD) (Jobin-Yvon Triax 320 Spectrometer) with a spectral resolution of $\sim$0.1 nm for spectral output measurement. Fig. 6 shows the emission intensity at RT from the hybrid GaN-based VCSEL as a function of the excitation energy. A distinct threshold characteristic can be found at the threshold excitation energy of $\sim$55 nJ corresponding to an energy density of 7.8 mJ/cm^2. Then, the laser output increased linearly with the pumping energy beyond the threshold. A dominant laser emission line at 448.9 nm appears above the threshold pumping energy. The threshold density of this hybrid DBR VCSEL is relatively lower than that of our previous report [28], which may originate from the improvement of the reflectivity of the epitaxially grown AlN/GaN-based DBR inserted with SL layers. The laser emission spectral linewidth reduces as the pumping energy rises above the threshold energy, and approaches 0.17 nm at the pumping energy of 82.5 nJ. In order to extract the spontaneous coupling factor β of this cavity from Fig. 6, we normalized the vertical scale and replotted it on a logarithm scale, as shown in the inset in Fig. 6. The difference between the heights of the emission intensities before and after the threshold roughly coincides with the value of β [46]. The β-value of this hybrid GaN-based VCSEL estimated from the inset of Fig. 6 is about 6×10^{-2}. The alternative approach to estimating the β-value is based on the approximation equation, which can be expressed by [47], [48]

$$\beta = \frac{F_p}{1 + F_p} \tag{1}$$

with

$$F_p = \frac{3}{4\pi^2} \frac{Q}{V_c/(\lambda/n)^3} \tag{2}$$

where F_p is the Purcell factor, Q is the cavity quality factor, λ is the laser wavelength, V_c is the optical volume of laser emission, and n is the refractive index. Since the PL spectrum of our hybrid DBR VCSEL showed a narrow emission peak with FWHM of 0.61 nm, the cavity quality factor was estimated to be 760. The refractive index is 2.45 for the GaN cavity. For the estimation of the optical volume, we used the spot size of the laser emission image that was about 3 μm and the cavity length of about 9.5λ while considering the penetration depth of the DBRs. By using these parameters, a Purcell factor of about 2.9×10^{-2} was obtained, and we estimated the β-value to be about 2.8×10^{-2}, which has the same order of magnitude as the previous β-value estimated from the inset in Fig. 6. This β-value is three orders of magnitude higher than that of the typical edge-emitting semiconductor lasers (normally about 10^{-4} to 10^{-5} [48]), indicating the enhancement of the spontaneous emission into a lasing mode by the high-quality-factor microcavity effect in the VCSEL structure. Fig. 7 shows the laser emission intensity as a function of the angle of the polarizer at the pumping energy

of 82.5 nJ. The variation of the laser emission intensity with the angle of the polarizer shows nearly a cosine square variation. The result shows that the laser beam has a degree of polarization of about 89%, suggesting a near-linear polarization property of the laser emission.

C. Characteristics of Electrically Pumped GaN-Based VCSEL

To fabricate the VCSEL structure for electrical excitation, additional processes for current injection are necessary. Since the epitaxially grown bottom AlN/GaN-based DBR was undoped and nonconductive, we processed the epitaxially grown wafer to form the intracavity coplanar p- and n-contacts for current injection. First, the mesa region was defined by photolithography and etched using an inductively coupled plasma reactive ion etching system with Cl_2/Ar as the etching gases to expose the n-GaN layer for the n-contact formation. Then, a 0.2-μm-thick SiN_x layer was used as the mask to form a current injection and light-emitting aperture of 10 μm in diameter, which then deposited an ITO as the transparent contact layer. Since the ITO locates just next to the VCSEL microcavity, the thickness of 240 nm corresponding to 1λ optical length ($\lambda = 460$ nm) has to be accurate to match the phase condition and reduce the microcavity antiresonance effect. The ITO was annealed at 525 °C under the nitrogen ambient to reduce the contact resistance as well as to increase transparency, thus reducing the internal cavity loss. A high transmittance of about 98.6% at $\lambda = 460$ nm was measured for the deposited ITO after annealing. Then, the metal contact layer was deposited by electron beam evaporation using Ti/Al/Ni/Au (20/150/20/1000 nm) and Ni/Au (20/1000 nm) as the n-type electrode and p-type electrode, respectively, to form coplanar intracavity contacts. Finally, an eight-pair Ta_2O_5/SiO_2 dielectric DBR (measured reflectivity of about 99% at $\lambda = 460$ nm) was deposited on top of the ITO layer to form the top DBR mirror and complete the full hybrid microcavity VCSEL device. Fig. 8(a) shows the schematic of hybrid GaN-based VCSEL structure. Fig. 8(b) shows the SEM image of the completed VCSEL devices. For VCSEL performance characterization, the fabricated VCSEL devices were diced into an individual device size of 120 μm × 150 μm and packaged into the TO-can. The packaged VCSEL device was mounted inside a cryogenic chamber for testing under the 77 K condition. Fig. 8(c) shows the optical microscopy image of a GaN-based VCSEL sample device at an injection current of 1 mA. We placed the GaN-based VCSEL sample inside a liquid-nitrogen-cooled chamber at 77 K and tested under CW current injection condition using a CW current source (Keithley 238). The emission light was collected by a 25-μm-diameter multimode fiber using a microscope with a 40× objective (numerical aperture = 0.6) and fed into the spectrometer (Triax 320). The system has a focal distance of 320 mm and a grating of 1800 g/mm with a spectral resolution of 0.15 nm. The output from the spectrometer was detected by a CCD to record the emission spectrum. The spatial resolution of the imaging system was about 1 μm as estimated by the diffraction limit of the objective lens. The cross-sectional (SEM) image of the whole hybrid VCSEL structure is shown in Fig. 9.

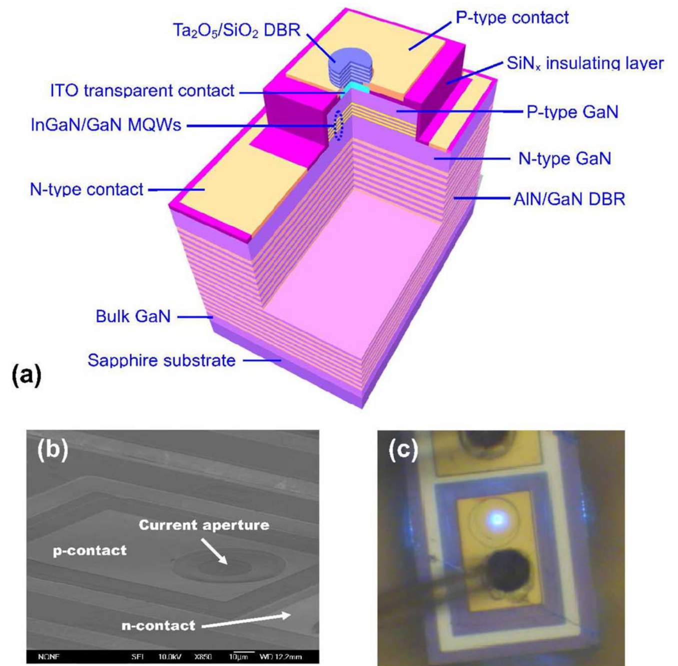

Fig. 8. Structure of electrically pumped hybrid GaN-based VCSEL. (a) Schematic diagram of the intracavity GaN-based VCSEL. (b) SEM image for the VCSEL with the intracavity with two co-planar p- and n-contacts for current injection. (c) Vertical surface emission image of a GaN-based VCSEL chip at an injection current of 1 mA. The crack line under the p-contact wire bond occurred during the chipping process.

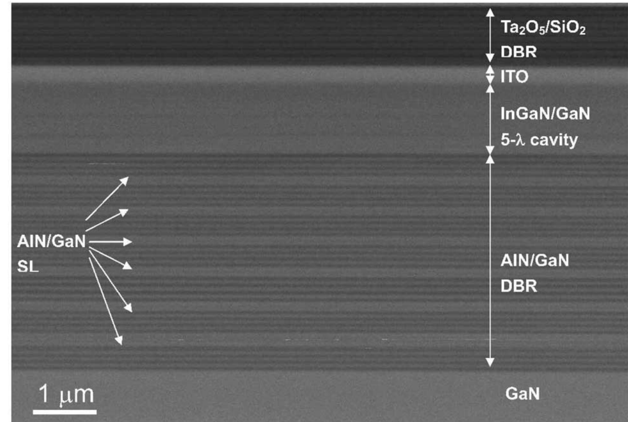

Fig. 9. Cross-sectional SEM image of the whole hybrid GaN-based VCSEL structure with hybrid DBRs, MQWs, and ITO layer.

Fig. 10(a) shows the reflectivity spectra of crack-free 29-pair AlN/GaN-based DBR with six SL insertion layers and eight-pair Ta_2O_5/SiO_2 DBR, respectively. A high peak reflectivity of 99.4% with a spectral bandwidth of ~25 nm was observed from the 29-pair AlN/GaN-based DBR. The flat-topped stopband indicates the high crystal quality of the AlN/GaN-based DBRs. The eight-pair Ta_2O_5/SiO_2 DBR shows a peak reflectivity of about 99% at 460 nm. The hybrid microcavity quality factor Q of the fabricated GaN-based VCSEL without the ITO layer was estimated from the PL spectrum of the VCSEL structure, as shown in Fig. 10(b). The VCSEL structure was also excited by a CW 325 nm He–Cd laser with a laser spot size of about

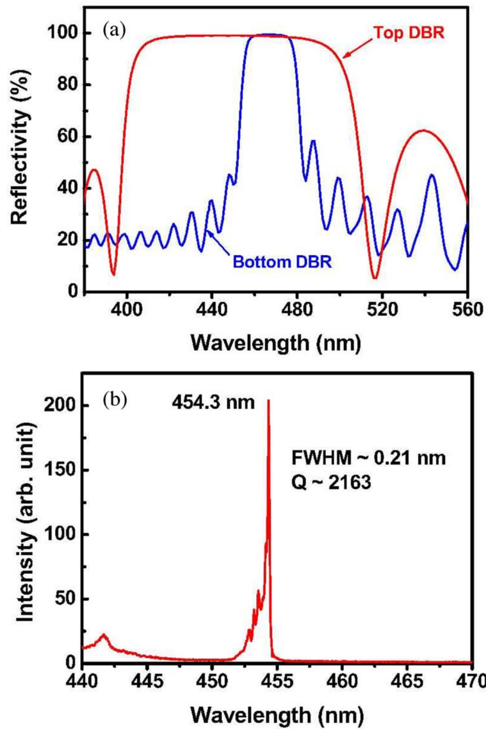

Fig. 10. (a) Reflectivity spectra of top and bottom DBRs show that the highest peak reflectivity of bottom and top DBR is about 99.4% and 99%, respectively. (b) PL spectrum of the GaN-based VCSEL structure excited by a CW He–Cd laser (325 nm) at RT.

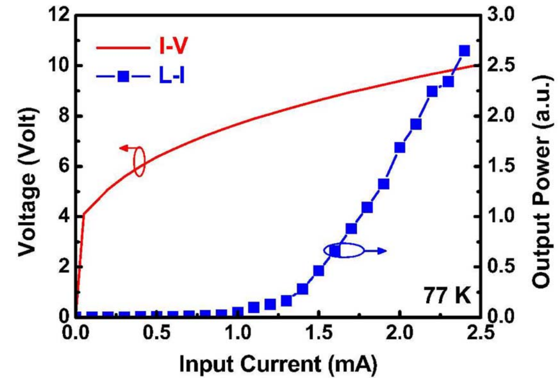

Fig. 11. Light output intensity versus injection current and current–voltage characteristics of GaN-based VCSEL measured under the CW condition at 77K.

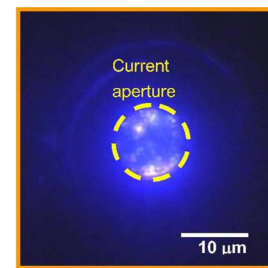

Fig. 12. Nonuniform current injection within the 10-μm current aperture below the threshold.

1 μm in diameter. From the PL emission peak of 454.3 nm and a narrow linewidth of 0.21 nm, we estimated the cavity Q-factor by $\lambda/\Delta\lambda$ to be about 2.2×10^3. This Q-value is larger than that of the previous optically pumped VCSEL structure, which may originate from the improvement of AlN/GaN-based DBR reflectivity and better sample quality. On the other hand, the Q-value is slightly higher than the value obtained from the whole VCSEL structure with intracavity ITO contact layer due to the additional absorption loss of the ITO.

Fig. 11 shows the light output power versus injection current and current–voltage characteristics (typical L–I–V characteristics of a laser) of the VCSEL sample at 77 K. The turn-on voltage is about 4.1 V, indicating the good electrical contact of the ITO transparent layer and the intracavity structure. The serial resistance of the VCSEL is about 1200 Ω at the driving current of 2.5 mA due to the small current injection aperture. The laser light output power showed a distinct threshold characteristic at the threshold current ($I_{\rm th}$) of about 1.4 mA, and then increased linearly with the injection current beyond the threshold. The threshold current density is estimated to be about 1.8 kA/cm^2 for a current injection aperture of 10 μm in diameter. The corresponding threshold carrier density is about 2.6×10^{19} cm^{-3}, estimated by assuming that the carrier lifetime of InGaN MQW is 6.4 ns and the internal quantum efficiency is 0.9 at 77 K [49]. However, from the spatial nonuniformity in the emission intensity as shown in Fig. 12 [27], the injected carriers are not uniformly spreading over the whole 10-μm current aperture. The actual area for carrier localizations appearing as these bright spots in the current aperture should be much smaller than the 10-μm current aperture. We estimated the carrier localization area to be about 30%–50% of the total aperture. Then, the carrier density for the lasing spots should be in the range of 5.2×10^{19} to 8.7×10^{19} cm^{-3}. We also estimated the threshold gain coefficient ($g_{\rm th}$) of our current injection in VCSEL operated at 77 K using the following equation:

$$g_{\rm th} \geq \frac{L_{\rm eff} - d_a}{d_a}\langle\alpha_i\rangle + \frac{1}{2d_a}\ln\left(\frac{1}{R_1 R_2}\right) \quad (3)$$

where $L_{\rm eff}$ is the effective cavity length, $\langle\alpha_i\rangle$ is the average internal loss inside the cavity, d_a is the total thickness of the MQW, and R_1 and R_2 are the reflectivities of the top and bottom DBR mirrors, respectively. Since the internal loss inside the cavity mainly came from the ITO absorption, we obtained a threshold gain coefficient value of about 8.8×10^3 cm^{-1}, which is a reasonable value for the carrier density in the range of 5.2×10^{19} to 8.7×10^{19} cm^{-3}.

Fig. 13 shows the laser emission spectrum at various injection current levels. A dominant single laser emission line at 462.8 nm appears above the threshold current. The inset in Fig. 13 shows the light emission linewidth at various injection current levels. The laser emission spectral linewidth reduces suddenly with the injection current above the threshold current and approaches the spectral resolution limit of 0.15 nm at the injection current of $1.7I_{\rm th}$. Another inset in Fig. 13 shows the CCD image of the spatial laser emission pattern across the 10 μm emission aperture at slightly below the threshold injection current of 1 mA. The nonuniform emission intensity across the emission

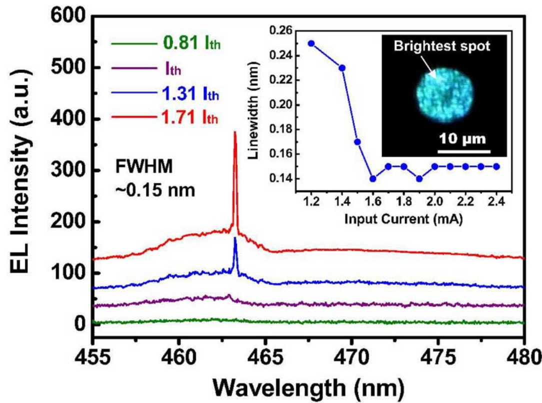

Fig. 13. Laser emission spectrum at different injection current levels measured at 77 K. (Inset) Light emission linewidth at various injection current levels and the CCD image of the emission from the aperture.

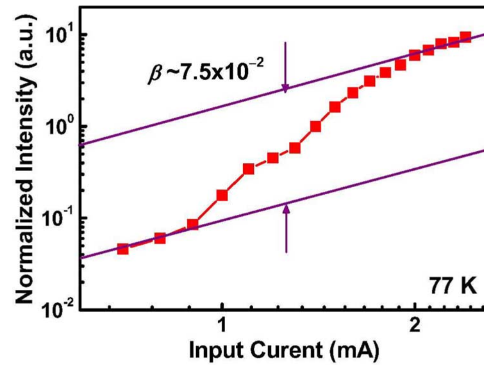

Fig. 14. Logarithm light output intensity as a function of input current at 77 K. The two solid lines are guides for the eye.

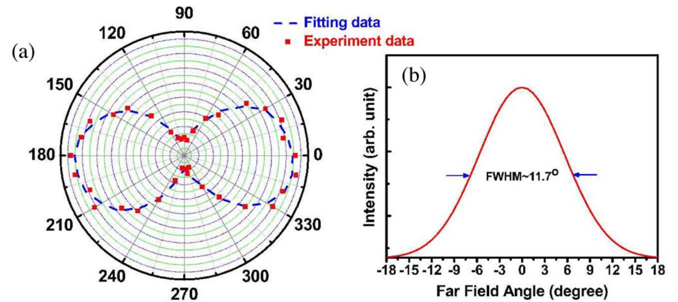

Fig. 15. (a) Polarization characteristics of the laser emission from the GaN-based VCSEL at the threshold. The experiment data are symbolized by dots and the blue dashed line is the fitting result. (b) FFP of the laser spot at the threshold. The divergence angle was estimated to be around 11.7°.

aperture with several bright emission spots was observed. The earlier report showed that InGaN MQWs tend to have indium inhomogeneity [50]; thus, we believe that the nonuniformity in the emission intensity across the aperture could be due to the indium nonuniformity that creates nonuniform spatial gain distribution in the emitting aperture. Actually, we observed that the lasing action mainly arises from the spots with brightest intensity, as indicated in the inset of Fig. 13. The spatial dimension of these bright spot clusters is only about few micrometers in diameter. A similar result was also observed and reported recently for the optically pumped GaN-based VCSELs [27]. Furthermore, we estimated the spontaneous emission coupling factor β of our VCSEL sample from Fig. 14, which is the logarithm plot of Fig. 11. The extracted β-value is about 7.5×10^{-2} for our GaN-based VCSEL. We also estimated the β-value from the Purcell factor F_p using the approximation equation as shown in (1) and (2). The cavity Q-value is about 1.8×10^3 based on the emission linewidth of 0.25 nm near the threshold. The optical volume V_c is estimated to be about 1.2×10^{-11} cm^3 for an emission spot size of about 3 μm. The cavity length is about 10.5λ considering the thickness of the ITO and the penetration depth of the DBRs. By using these parameters, we obtained a Purcell factor of about 7.9×10^{-2} and an estimated β-value of about 7.4×10^{-2}, which is close to the value obtained previously from Fig. 14. This high β-value of our microcavity VCSEL could be responsible for low-threshold operation of our laser. Fig. 15 shows the polarization characteristics and far-field pattern (FFP) of the laser emission. The laser emission has a degree of polarization of about 80% and the FWHM of the FFP is about 11.7° in both horizontal and vertical directions.

IV. Perspectives

The lasing action of GaN-based hybrid DBR VCSEL by optical pumping at RT and CW electrical pumping at 77 K was demonstrated. The next challenge of GaN-based VCSEL is to achieve RT CW operation. The difficulties for our VCSEL structure to achieve RT CW operation may be due to several important issues. The current crowding in the intracavity-contacted structure is an important problem that induces a high operation voltage and heat generation. It is well known that the performance of the semiconductor laser will degrade with the increasing device temperature because of the broadening of the gain spectra, increased nonradiative recombination, and carrier leakage. These heat-induced problems are especially serious in nitride-based VCSELs due to the relatively large thermal resistance in multilayer DBR and the smaller size of current aperture [51], and QCSE-induced electron current leakage [52]. In addition, heat dissipation limited by the poor thermal conductivity of the sapphire substrate significantly affects the device performance. These issues should be the main physical mechanisms limiting the lasing action observed at 77 K. The advanced design for improving the operation temperature of GaN-based VCSELs will employ the AlGaN electronic blocking layer after the growth of MQWs, which can effectively suppress the electron leakage current [53]. Furthermore, it has been reported that the use of polarization-matched InGaN/AlInGaN MQWs enables an independent control over interface polarization charges and bandgap, and has been suggested as a method to reduce electron leakage current [54]. On the other hand, conventional GaAs-based VCSELs mostly use the wet oxidation technique to achieve effective index-guiding structures. However, the design of intracavity structure has the problem of effective confinement of an optical field in a radial direction of standard nitride-based VCSELs [55]. Furthermore, several technical issues should be considered. These include the design of a transparent and good current spreading contact structure for carrier injection, improvement of the spatial uniformity of InGaN MQW active

region because of relatively small light emission aperture of the current injection device, enhancement of p-type GaN layer conductivity, and further increase of the high reflectivity of DBRs for the reduction of threshold current. It is necessary to overcome these problems to achieve the RT CW GaN-based VCSELs.

V. Summary

We have reviewed the development of GaN-based VCSELs from optical pumping to electrical pumping. For the hybrid DBR VCSELs, we have fabricated a crack-free, high-reflectivity AlN/GaN-based DBR by insertion of SL layers and use the high-reflective Ta_2O_5/SiO_2 as dielectric mirror, and achieved laser operation under optical pumping at RT. The optically pumped laser has a threshold energy of 55 nJ and a high degree of polarization of 89%. The high spontaneous emission coupling factor of 6×10^{-2} is estimated from the approximation equations. Furthermore, we fabricated and demonstrated the first CW operation of an electrically pumped GaN-based VCSEL at 77 K based on the previous optically pumped hybrid VCSEL structure. CW laser action occurred at a threshold current of 1.4 mA with an emission wavelength at 462.8 nm in blue wavelength at 77 K. The laser beam has a low divergence angle of about 11.7° and a degree of polarization of about 80%. The laser shows a strong spontaneous emission coupling with an estimated coupling efficiency of about 7.5×10^{-2}. A nonuniform spatial laser intensity emission pattern was also observed from the CCD image. Although the lasing action of electrically pumped GaN-based VCSEL has been observed at 77 K, there are still few technical issues and advanced structure design that need to be resolved before the RT CW GaN-based VCSEL can be realized. It is expected that the successful operation of electrically pumped GaN-based VCSELs at 77 K is a useful and helpful guide for the design and fabrication of RT CW electrically pumped GaN-based VCSELs in the near future.

References

[1] H. Amano, M. Kito, K. Hiramatsu, and I. Akasaki, "P-type conduction in Mg-doped GaN treated with low-energy electron beam irradiation (LEEBI)," *Jpn. J. Appl. Phys*, vol. 28, pp. L2112–L2114, 1989.

[2] I. Akasaki, H. Amano, K. Itoh, N. Koide, and K. Manabe, "GaN based UV/blue light-emitting devices," in *Proc. Inst. Phys. Conf. Ser.*, 1992, vol. 129, pp. 851–856.

[3] S. Nakamura, T. Mukai, and M. Senoh, "Candela-class high-brightness InGaN/AlGaN double-heterostructure blue-light-emitting diodes," *Appl. Phys. Lett.*, vol. 64, pp. 1687–1689, 1994.

[4] S. Nakamura, M. Senoh, S.-I. Nagahama, N. Iwasa, T. Yamada, T. Matsushita, Y. Sugimoto, and H. Kiyoku, "Room-temperature continuous-wave operation of InGaN multi-quantum-well structure laser diodes," *Appl. Phys. Lett.*, vol. 69, pp. 4056–4058, 1996.

[5] S. Nakamura, M. Senoh, S.-I. Hagahama, N. Iwasa, T. Yamada, T. Matsushita, H. Kiyoku, Y. Sugimoto, T. Kozaki, H. Umemoto, M. Sano, and K. Chocho, "High-power, long-lifetime InGaN/GaN/AlGaN-based laser diodes grown on pure GaN substrates," *Jpn. J. Appl. Phys*, vol. 37, pp. L309–L312, 1998.

[6] S. Nakamura, M. Senoh, S.-I. Nagahama, N. Iwasa, T. Yamada, T. Matsushita, H. Kiyoku, Y. Sugimoto, T. Kozaki, H. Umemoto, M. Sano, and K. Chocho, "Violet InGaN/GaN/AlGaN-based laser diodes with an output power of 420 mW," *Jpn. J. Appl. Phys.*, vol. 37, pp. L627–L629, 1998.

[7] S. Nakamura, M. Senoh, and T. Mukai, "Highly p-typed Mg-doped GaN films grown with GaN buffer layers," *Jpn. J. Appl. Phys.*, vol. 30, pp. L1708–L1711, 1991.

[8] S. Nakamura, N. Iwasa, M. Senoh, and T. Mukai, "Hole compensation mechanism of p-type GaN films," *Jpn. J. Appl. Phys.*, vol. 31, pp. 1258–1266, 1992.

[9] K. Iga, "Surface-emitting laser—Its birth and generation of new optoelectronics field," *IEEE J. Sel. Topics Quantum Electron.*, vol. 6, no. 6, pp. 1201–1215, Nov. 2000.

[10] W. W. Chow, K. D. Choquette, M. H. Crawford, K. L. Lear, and G. R. Hadley, "Design, fabrication, and performance of infrared and visible vertical-cavity surface-emitting lasers," *IEEE J. Quantum Electron.*, vol. 33, no. 10, pp. 1810–1824, Oct. 1997.

[11] E. Towe, R. F. Leheny, and A. Yang, "A historical perspective of the development of the vertical-cavity surface-emitting laser," *IEEE J. Sel. Topics Quantum Electron.*, vol. 6, no. 6, pp. 1458–1464, Nov./Dec. 2000.

[12] F. Semond, I. R. Sellers, F. Natali, D. Byrne, M. Leroux, J. Massies, N. Ollier, J. Leymarie, P. Disseix, and A. Vasson, "Strong light–matter coupling at room temperature in simple geometry GaN microcavities grown on silicon," *Appl. Phys. Lett.*, vol. 87, pp. 021102-1–021102-3, 2005.

[13] R. Butté, G. Christmann, E. Feltin, J.-F. Carlin, M. Mosca, M. Ilegems, and N. Grandjean, "Room-temperature polariton luminescence from a bulk GaN microcavity," *Phys. Rev. B*, vol. 73, pp. 033315-1–033315-4, 2006.

[14] G. Christmann, R. Butté, E. Feltin, J.-F. Carlin, and N. Grandjean, "Impact of inhomogeneous excitonic broadening on the strong exciton–photon coupling in quantum well nitride microcavities," *Phys. Rev. B*, vol. 73, pp. 153305-1–153305-4, 2006.

[15] S. Kako, C. Santori, K. Hoshino, S. Götzinger, Y. Yamamoto, and Y. Arakawa, "A gallium nitride single-photon source operating at 200 K," *Nat. Mater.*, vol. 5, pp. 887–892, 2006.

[16] S. Christopoulos, G. von Högersthal, A. Grundy, P. G. Lagoudakis, A. V. Kavokin, J. J. Baumberg, G. Christmann, R. Butté, E. Feltin, J.-F. Carlin, and N. Grandjean, "Room-temperature polariton lasing in semiconductor microcavities," *Phys. Rev. Lett.*, vol. 98, pp. 126405-1–126405-4, 2007.

[17] J. M. Redwing, D. A. S. Loeber, N. G. Anderson, M. A. Tischler, and J. S. Flynn, "An optically pumped GaN–AlGaN vertical cavity surface emitting laser," *Appl. Phys. Lett.*, vol. 69, pp. 1–3, 1996.

[18] T. Someya, K. Tachibana, J. Lee, T. Kamiya, and Y. Arakawa, "Lasing emission from an $In_0.1Ga_0.9N$ vertical cavity surface emitting laser," *Jpn. J. Appl. Phys.*, vol. 37, pp. L1424–L1426, 1998.

[19] Y.-K. Song, H. Zhou, M. Diagne, I. Ozden, A. Vertikov, A. V. Nurmikko, C. Carter-Coman, R. S. Kern, F. A. Kish, and M. R. Krames, "A vertical cavity light emitting InGaN quatnum well heterostructure," *Appl. Phys. Lett.*, vol. 74, pp. 3441–3443, 1999.

[20] T. Someya, R. Werner, A. Forchel, M. Catalano, R. Cingolani, and Y. Arakawa, "Room temperature lasing at blue wavelengths in gallium nitride microcavities," *Science*, vol. 285, pp. 1905–1906, 1999.

[21] J.-F. Carlin, J. Dorsaz, E. Feltin, R. Butté, N. Grandjean, M. Ilegems, and M. Laügt, "Crack-free fully epitaxial nitride microcavity using highly reflective AlInN/GaN Bragg mirrors," *Appl. Phys. Lett.*, vol. 86, pp. 031107-1–031107-3, 2005.

[22] H. Zhou, M. Diagne, E. Makarona, A. V. Nurmikko, J. Han, K. E. Waldrip, and J. J. Figiel, "Near ultraviolet optically pumped vertical cavity laser," *Electron. Lett.*, vol. 36, pp. 1777–1779, 2000.

[23] S.-H. Park, J. Kim, H. Jeon, T. Sakong, S.-N. Lee, S. Chae, Y. Park, C.-H. Jeong, G.-Y. Yeom, and Y.-H. Cho, "Room-temperature GaN vertical-cavity surface-emitting laser operation in an extended cavity scheme," *Appl. Phys. Lett.*, vol. 83, pp. 2121–2123, 2003.

[24] T. Tawara, H. Gotoh, T. Akasaka, N. Kobayashi, and T. Saitoh, "Low-threshold lasing of InGaN vertical-cavity surface-emitting lasers with dielectric distributed Bragg reflectors," *Appl. Phys. Lett.*, vol. 83, pp. 830–832, 2003.

[25] E. Feltin, G. Christmann, J. Dorsaz, A. Castiglia, J.-F. Carlin, R. Butté, N. Grandjean, S. Christopoulos, G. Baldassarri, H. von Högersthal, A. J. D. Grundy, P. G. Lagoudakis, and J. J. Baumberg, "Blue lasing at room temperature in an optically pumped lattice-matched AlInN/GaN VCSEL structure," *Electron. Lett.*, vol. 43, pp. 924–926, 2007.

[26] J.-T. Chu, T.-C. Lu, H.-H. Yao, C.-C. Kao, W.-D. Liang, J.-Y. Tsai, H.-C. Kuo, and S.-C. Wang, "Room-temperature operation of optically pumped blue-violet GaN-based vertical-cavity surface-emitting lasers fabricated by laser lift-off," *Jpn. J. Appl. Phys*, vol. 45, pp. 2556–2560, 2006.

[27] J.-T. Chu, T.-C. Lu, M. You, B.-J. Su, C.-C. Kao, H.-C. Kuo, and S.-C. Wang, "Emission characteristics of optically pumped GaN-based vertical-cavity surface-emitting lasers," *Appl. Phys. Lett.*, vol. 89, pp. 121112-1–121112-3, 2006.

[28] C.-C. Kao, Y. C. Peng, H. H. Yao, J. Y. Tsai, Y. H. Chang, J. T. Chu, H. W. Huang, T. T. Kao, T. C. Lu, H. C. Kuo, and S. C. Wang, "Fabrication

and performance of blue GaN-based vertical-cavity surface emitting laser employing AlN/GaN and Ta_2O_5/SiO_2 distributed Bragg reflector," *Appl. Phys. Lett.*, vol. 87, pp. 081105-1–081105-3, 2005.
[29] C.-C. Kao, T. C. Lu, H. W. Huang, J. T. Chu, Y. C. Peng, H. H. Yao, J. Y. Tsai, T. T. Kao, H. C. Kuo, S. C. Wang, and C. F. Lin, "The lasing characteristics of GaN-based vertical-cavity surface-emitting laser with AlN–GaN and Ta_2O_5–SiO_2 distributed Bragg reflectors," *IEEE Photon. Technol. Lett.*, vol. 18, no. 7, pp. 877–879, 2006.
[30] S.-C. Wang, T.-C. Lu, C.-C. Kao, J.-T. Chu, G.-S. Huang, H.-C. Kuo, S.-W. Chen, T.-T. Kao, J.-R. Chen, and L.-F. Lin, "Optically pumped GaN-based vertical cavity surface emitting lasers: Technology and characteristics," *Jpn. J. Appl. Phys.*, vol. 46, pp. 5397–5407, 2007.
[31] T.-C. Lu, C.-C. Kuo, H.-C. Kuo, G.-S. Huang, and S.-C. Wang, "CW lasing of current injection blue GaN-based vertical cavity surface emitting laser," *Appl. Phys. Lett.*, vol. 92, pp. 141102-1–141102-3, 2008.
[32] F. A. Ponce and D. P. Bour, "Nitride-based semiconductors for blue and green light-emitting devices," *Nature*, vol. 386, pp. 351–359, 1997.
[33] J. Li, T. N. Oder, M. L. Nakarmi, J. Y. Lin, and H. X. Jiang, "Optical and electrical properties of Mg-doped p-type $Al_xGa_{1-x}N$," *Appl. Phys. Lett.*, vol. 80, pp. 1210–1212, 2002.
[34] E. Petrolati and A. D. Carlo, "The influence of mobility unbalance on GaN based vertical cavity surface emitting lasers," *Appl. Phys. Lett.*, vol. 92, pp. 151116-1–151116-3, 2008.
[35] S. Chichibu, T. Azuhata, T. Sota, and S. Nakamura, "Spontaneous emission of localized excitons in InGaN single and multiquantum well structures," *Appl. Phys. Lett.*, vol. 69, pp. 4188–4190, 1996.
[36] J.-F. Carlin and M. Ilegems, "High-quality AlInN for high index contrast Bragg mirrors lattice matched to GaN," *Appl. Phys. Lett.*, vol. 83, pp. 668–670, 2003.
[37] T. Fujimori, H. Imai, A. Wakahara, H. Okada, A. Yoshida, T. Shibata, and M. Tanaka, "Growth and characterization of AlInN on AlN template," *J. Cryst. Growth*, vol. 272, pp. 381–385, 2004.
[38] R. Butté, E. Feltin, J. Dorsaz, G. Christmann, J.-F. Carlin, N. Grandjean, and M. Ilegems, "Recent progress in the growth of highly reflective intride-based distributed Bragg reflectors and their use in microcavities," *Jpn. J. Appl. Phys.*, vol. 44, pp. 7207–7216, 2005.
[39] G. S. Huang, T. C. Lu, H. H. Yao, H. C. Kuo, S. C. Wang, C.-W. Lin, and L. Chang, "Crack-free GaN/AlN distributed Bragg reflectors incorporated with GaN/AlN superlattices grown by metalorganic chemical vapor deposition," *Appl. Phys. Lett.*, vol. 88, pp. 061904-1–061904-3, 2006.
[40] H. K. Cho, J. Y. Lee, and G. M. Yang, "Characterization of pit formation in III-nitrides grown by metalorganic chemical vapor deposition," *Appl. Phys. Lett.*, vol. 80, pp. 1370–1372, 2002.
[41] S. Einfeldt, H. Heinke, V. Kirchner, and D. Hommel, "Strain relaxation in AlGaN/GaN superlattices grown on GaN," *Appl. Phys. Lett.*, vol. 89, pp. 2160–2167, 2001.
[42] K. Iga, "Possibility of green/blue/UV surface emitting lasers," in *Proc. Int. Symp. Blue Laser Light Emitting Diodes*, Mar., 1996, Paper Th-11, pp. 263–266.
[43] X. H. Zhang, S. J. Chua, W. Liu, L. S. Wang, A. M. Yong, and S. Y. Chow, "Crack-free fully epitaxial nitride microcavity with AlGaN/GaN distributed Bragg reflectors and InGaN/GaN quantum wells," *Appl. Phys. Lett.*, vol. 88, pp. 191111-1–191111-3, 2006.
[44] H. Benisty, H. De Neve, and C. Weisbuch, "Impact of planar microcavity effects on light extraction—Part I: Basic concepts and analytical trends," *IEEE J. Quantum Electron.*, vol. 34, no. 9, pp. 1612–1631, Sep. 1998.
[45] H. Benisty, H. De Neve, and C. Weisbuch, "Impact of planar microcavity effects on light extraction—Part II: Selected exact simulations and role of photon recycling," *IEEE J. Quantum Electron.*, vol. 34, no. 9, pp. 1632–1643, Sep. 1998.
[46] R. J. Horowicz, H. Heitmann, Y. Kadota, and Y. Yamamoto, "GaAs microcavity quantum-well laser with enhanced coupling of spontaneous emission to the lasing mode," *Appl. Phys. Lett.*, vol. 61, pp. 393–395, 1992.
[47] Y. Yamamoto and S. Machida, "Microcavity semiconductor laser with enhanced spontaneous emission," *Phys. Rev. A.*, vol. 44, pp. 657–668, 1991.
[48] S. Kako, T. Someya, and Y. Arakawa, "Observation of enhanced spontaneous emission coupling factor in nitride-based vertical-cavity surface-emitting laser," *Appl. Phys. Lett.*, vol. 80, pp. 722–724, 2002.
[49] A. Kaneta, K. Okamoto, Y. Kawakami, S. Fujita, G. Marutsuki, Y. Narukawa, and T. Mukai, "Spatial and temporal luminescence dynamics in an In_xGa_1N single quantum well probed by near-field optical microscopy," *Appl. Phys. Lett.*, vol. 81, pp. 4353–4355, 2002.
[50] B. Witzigmann, V. Laino, M. Luisier, U. T. Schwarz, G. Feicht, W. Wegscheider, K. Engl, M. Furitsch, A. Leber, A. Lee, and V. Härle, "Microscopic analysis of optical gain in InGaN/GaN quantum wells," *Appl. Phys. Lett.*, vol. 88, pp. 021104-1–021104-3, 2006.
[51] M. H. MacDougal, P. D. Dapkus, A. E. Bond, C.-K. Lin, and J. Geske, "Design and fabrication VCSEL's with Al_xO_y–GaAs DBR's," *IEEE J. Sel. Topics Quantum Electron.*, vol. 3, no. 3, pp. 905–915, Jun. 1997.
[52] J. Piprek, R. Farrell, S. DenBaars, and S. Nakamura, "Effects of built-in polarization on InGaN–GaN vertical-cavity surface-emitting lasers," *IEEE Photon. Technol. Lett.*, vol. 18, no. 1, pp. 7–9, Jan. 2006.
[53] Y.-K. Kuo and Y.-A. Chang, "Effects of electronic current overflow and inhomogeneous carrier distribution on InGaN quantum-well laser performance," *IEEE J. Quantum Electron.*, vol. 40, no. 5, pp. 437–444, Jan. 2006.
[54] M. F. Schubert, J. Xu, J. K. Kim, E. F. Schubert, M. H. Kim, S. Yoon, S. M. Lee, C. Sone, T. Sakong, and Y. Park, "Polarization-matched GaInN/AlGaInN multi-quantum-well light-emitting diodes with reduced efficiency droop," *Appl. Phys. Lett.*, vol. 93, pp. 041102-1–041102-3, 2008.
[55] P. Maćkowiak, R. P. Sarzała, M. Wasiak, and W. Nakwaski, "Nitride VCSEL design for continuous-wave operation of higher-order optical modes," *Appl. Phys. A*, vol. 77, pp. 761–768, 2003.

Tien-Chang Lu (M'07) received the B.S. degree in electrical engineering from the National Taiwan University, Taipei, Taiwan, in 1995, the M.S. degree in electrical engineering from the University of Southern California, Los Angeles, in 1998, and the Ph.D. degree in electrical engineering and computer science from the National Chiao Tung University (NCTU), Hsinchu, Taiwan, in 2004.

During 2004, he was the Manager of the Epitaxy Department, Union Optronics Corporation. Since August 2005, he has been a member of the faculty in the Department of Photonics, NCTU. His current research interests include the design, epitaxial growth, process, and characterization of optoelectronic devices such as Fabry–Perot type semiconductor lasers, vertical-cavity surface-emitting lasers, resonant-cavity LEDs, wafer-fused flip-chip LEDs, solar cells, etc. He has also been engaged in the low-pressure metal–organic chemical vapor deposition (MOCVD) epitaxial technique associated with various material systems including InGaAlAs, InGaAsP, AlGaAs, InGaAlP, and InGaAlN as well as the corresponding process skills. He is also involved in the structure design and simulations for optoelectronic devices using computer-aided software. He has authored or coauthored more than 80 internal journal papers.

Prof. Lu was a recipient of the Exploration Research Award of the Pan Wen Yuan Foundation in 2007 and the Excellent Young Electronic Engineer Award in 2008.

Jun-Rong Chen was born in Taichung, Taiwan, on October 23, 1980. He received the B.S. degree in physics from the National Changhua University of Education (NCUE), Changhua, Taiwan, in 2004, and the M.S. degree in optoelectronics from the Institute of Photonics, NCUE, in 2006. He is currently working toward the Ph.D. degree at the Department of Photonics and the Institute of Electro-Optical Engineering, National Chiao Tung University (NCTU), Hsinchu, Taiwan.

In 2006, he was with the Semiconductor Laser Technology Laboratory, NCTU, where he was engaged in research on III–V semiconductor materials for LEDs and semiconductor lasers. His current research interests include III-nitride semiconductor lasers, epitaxial growth of III-nitride materials, and numerical simulation of III–V optoelectronic devices.

Shih-Wei Chen received the B.S. degree in electrical engineering and the M.S. degree in optoelectronic sciences from the National Taiwan Ocean University (NTOU), Keelung, Taiwan, in 2004 and 2006, respectively. He is currently working toward the Ph.D. degree in electrooptical engineering at the National Chiao-Tung University, Hsinchu, Taiwan.

In 2006, he joined the Semiconductor Laser Technology Laboratory, National Chiao-Tung University. His current research interests include LEDs, GaN vertical-cavity surface-emitting laser (VCSEL), high-Q microcavity LED, and photonic crystal surface-emitting lasers that can be applied to short-range fiber optical communication such as gigabit Ethernet and fiber channel.

Hao-Chung Kuo (S'98–M'99–SM'06) received the B.S. degree in physics from the National Taiwan University, Taipei, Taiwan, in 1990, the M.S. degree in electrical and computer engineering from Rutgers University, Camden, NJ, in 1995, and the Ph.D. degree in electrical and computer engineering from the University of Illinois at Urbana-Champaign, Urbana, Illinois, in 1999.

He has an extensive professional career both in research and industrial research institutions. From 1995 to 1997, he was a Research Consultant with Lucent Technologies, Bell Lab, Holmdel, NJ. From 1999 to 2001, he was an R&D Engineer with the Fiber-Optics Division, Agilent Technologies. From 2001 to 2002, he was the R&D Manager with LuxNet Corporation. Since September 2002, he has been a member of the faculty at the Institute of Electro-Optical Engineering, National Chiao Tung University (NCTU), Hsinchu, Taiwan. He has authored or coauthored over 60 publications. His current research interests include the epitaxy, design, fabrication, and measurement of high-speed InP- and GaAs-based vertical-cavity surface-emitting lasers, as well as GaN-based lighting-emitting devices and nanostructures.

Chien-Cheng Kuo was born in Tainan, Taiwan, on July 11, 1974. He received the B.S. degree in physics from the National Cheng Kung University (NCKU), Tainan, Taiwan, in 1996, and the M.S. and Ph.D. degrees from the Institute of Optical Sciences, National Central University (NCU), Jhongli, Taiwan, in 1998 and 2007, respectively.

From 2000 to 2002, he was the Manager of the Manufacture Department, YCL OptoCom. Since 2007, he has been a Postdoctoral Research Fellow with the Thin Film Technology Center, NCU. His current research interests include optical thin films, dense wavelength division multiplexed (DWDM) optical thin-film filter, projector optical thin-film filter, and vacuum system.

Cheng-Chung Lee received the B.S. and M.S. degrees in physics from the National Cheng Kung University (NCKU), Tainan, Taiwan, in 1969 and 1974, respectively, and the Ph.D. degree from the Optical Sciences Center, University of Arizona, Tucson, in 1983.

He is the Chair of the Department of Optics and Photonics and the Director of the Thin Film Technology Center, National Central University (NCU), Jhongli, Taiwan. His current research interests include the fundamental investigation and application of optical thin films. He has also done coatings for optical communication (near IR), interference filters for periodically time-varying (PTV) (visible), optical coatings for lithography [UV and extreme UV (EUV)], and coating for color display and nanostructured thin film for optical applications such as color display and solar cell. He has also been engaged in the modification of coater, filter design, fabrication, and testing setup for his research and coating industries in Taiwan, Japan, and USA. He has authored or coauthored more than 100 International journal papers and more than 200 conference papers including some invited talks.

Prof. Lee is an Advisor of the NCU International Society for Optical Engineers (SPIE) and Optical Society of America (OSA) Student Chapter. He is also a Fellow of the SPIE and the OSA. In 2005, he was honored as a Distinguished Professor for his distinguished academic performance and outstanding research contributions.

Shing-Chung Wang (M'79–SM'03–LM'07) received the B.S. degree from the National Taiwan University, Taipei, Taiwan, the M.S. degree from the National Tohoku University, Sendai, Japan, and the Ph.D. degree from Stanford University, Stanford, CA, in 1971, all in electrical engineering.

He has an extensive professional career both in academic and industrial research institutions. He was a member of the faculty at the National Chiao Tung University (NCTU), Hsinchu, Taiwan (from 1965 to 1967), a Research Associate with Stanford University (from 1971 to 1974), a Senior Research Scientist with Xerox Corporation (from 1974 to 1985), and a Consulting Scientist with Lockheed-Martin Palo Alto Research Laboratories (from 1985 to 1995). Since 1995, he has been a member of the faculty at the Institute of Electro-Optical Engineering, NCTU. He has authored or coauthored over 160 publications. His current research interests include semiconductor lasers, vertical-cavity surface-emitting lasers, blue and UV lasers, quantum-confined optoelectronic structures, optoelectronic materials, diode-pumped lasers, and semiconductor–laser applications.

Prof. Wang is a Fellow of the Optical Society of America and the recipient of the Outstanding Scholar Award from the Foundation for the Advancement of Outstanding Scholarship.